
LEC²O-NeRF: LEARNING CONTINUOUS AND COMPACT LARGE-SCALE OCCUPANCY FOR URBAN SCENES

Zhenxing Mi & Dan Xu

Department of Computer Science and Engineering
The Hong Kong University of Science and Technology (HKUST)
Clear Water Bay, Kowloon, Hong Kong
zmiaa@connect.ust.hk, danxu@cse.ust.hk

ABSTRACT

In Neural Radiance Fields (NeRFs), a critical problem is how to effectively estimate the occupancy to guide empty-space skipping and point sampling. The grid-based methods work well for small-scale scenes. However, on large-scale scenes, they are limited by predefined bounding boxes, grid resolutions, and high memory usage for grid updates, and thus struggle to speed up training for large-scale, irregularly bounded and complex urban scenes without sacrificing accuracy. In this paper, we propose to learn a continuous and compact large-scale occupancy network, which can classify 3D points as occupied or unoccupied points. We successfully train this occupancy network end-to-end together with the radiance field in a self-supervised manner by three core designs. *First*, we propose a novel imbalanced occupancy loss to regularize the occupancy network. It enables the occupancy network to effectively control the ratio of the unoccupied and occupied points, motivated by the prior that most of the 3D scene points are unoccupied. *Second*, we design an imbalanced network architecture containing a large scene network and a small empty space network to separately encode occupied and unoccupied points classified by the occupancy network. This imbalanced structure can effectively model the imbalanced nature of occupied and unoccupied regions. *Third*, we design an explicit density loss to guide the occupancy network, making the density of unoccupied points smaller. As far as we know, we are the first to learn a continuous and compact occupancy of large-scale NeRF by a network. We show in the experiments that our occupancy network can very quickly learn more compact, accurate and smooth occupancy compared to the occupancy grid. With our learned occupancy as guidance for empty space skipping on several challenging large-scale benchmarks, our method consistently obtains higher accuracy compared to the occupancy grid, and our method can successfully speed up state-of-the-art NeRF methods without sacrificing accuracy.

1 INTRODUCTION

Neural Radiance Fields (NeRF) (Mildenhall et al., 2020) have been used to model large-scale 3D scenes (Turki et al., 2022; Tancik et al., 2022; MI & Xu, 2023). Although achieving promising performances, the critical problem of modeling occupancy for large-scale scenes remains under-explored. A large 3D scene is usually very sparse, with a large portion of the 3D scene as empty spaces. Thus, modeling the occupancy can effectively guide the empty-space skipping and point sampling. Using an occupancy grid for guided sampling has become a common practice in small-scale NeRF (Müller et al., 2022; Fridovich-Keil et al., 2022; Hu et al., 2022; Li et al., 2022). As shown in Fig. 1, the occupancy grid stores momentum density and occupancy in its cells. During NeRF training, points are sampled from grid cells, and the grid’s density values are updated in a momentum-based manner by evaluating the NeRF model. Binary occupancy is determined by applying a threshold to the momentum density values. The computation of updating the grid is determined by the grid’s resolution, and a higher resolution leads to significantly increased overhead.

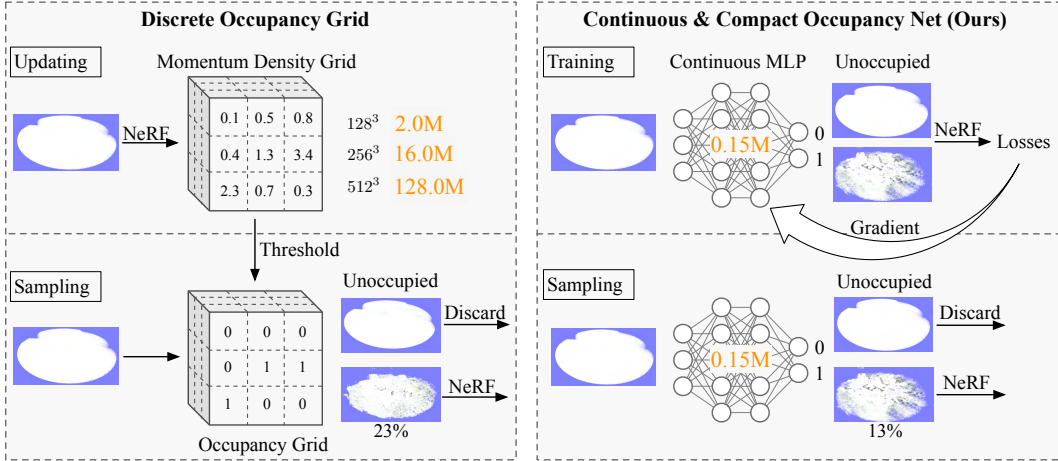


Figure 1: Differences between the occupancy grid (Li et al., 2022; Müller et al., 2022) and our occupancy network. Our occupancy network is a *compact and continuous* MLP with only 0.15M parameters, trained together with NeRF networks by our designed losses. The occupancy grid is a *discrete* representation and stores 2.0M and 128.0M parameters for a resolution of 128^3 and 512^3 , respectively. It is updated by evaluating the NeRF network and is not aware of the training loss. The images are the visualization of the occupied and unoccupied points as stated in Section 4.2. The whole points are sent to the grid or the occupancy network and are split into two parts of occupied and unoccupied points.

The occupancy grid works well on small-scale scenes while having clear limitations on large-scale scenes: **(i)** The memory and computation used to store and update the grid increase remarkably along with the grid’s resolution. This limits the grid from increasing its resolution to model detailed large-scale scenes. **(ii)** The occupancy grid needs more prior knowledge of the scene. The scene should be more regular so that it has a tight bounding box. **(iii)** Most of the grids are unoccupied due to the scene’s sparsity, making the grid not compact enough, thus wasting memory and computation. **(iv)** The momentum updating of the occupancy grid is not aware of the rendering loss, making it agnostic to the rendering quality, leading to unsatisfactory results. Due to these limitations, the occupancy grid fails to speed up the training of large-scale NeRF without sacrificing the accuracy in our experiments. Therefore, it is challenging to directly model the occupancy of large-scale complex scenes with the occupancy grid.

To tackle the challenges of modeling occupancy for large-scale scenes, in this paper, we propose LeC²O-NeRF to learn a continuous and compact occupancy representation by a network, depicted in Fig. 1. An essential nature of a 3D scene is that the occupied points are much fewer than the unoccupied points, while containing significantly more important information. Therefore, modeling occupancy is naturally very imbalanced. This motivates us to propose an imbalanced occupancy loss, an imbalanced network, and a density loss to successfully learn the occupancy. Our contributions are discussed below.

Firstly, we propose to learn the occupancy by a continuous and compact classification network. We train this network end-to-end and in a self-supervised manner together with the NeRF network. **Secondly**, we propose an imbalanced occupancy loss to regularize the occupancy network. Since a large portion of the 3D space is unoccupied, the occupancy network should explicitly model the imbalance of occupancy. We design an imbalanced occupancy loss to approximately control the portion of occupied and unoccupied points. We can use it to make only a small portion of the 3D points classified as occupied. **Thirdly**, we design an imbalanced network architecture to model the radiance field. It contains a large scene network for occupied points and a small empty space network for unoccupied points. The occupancy network works as a dispatcher to send points into different networks. A point is seen as unoccupied if the empty space network is selected for it. The empty space network contains much fewer parameters than the scene network, modeling the prior that the unoccupied points are less informative and much easier to encode. With the imbalanced occupancy loss and the imbalanced network architecture, we find that the occupancy network can

already distinguish the occupied and unoccupied points effectively. **Fourthly**, to better learn the occupancy of a large-scale scene, we propose a density loss to guide the training of the occupancy network. In a NeRF representation, the density of an unoccupied point is much smaller than that of an occupied point. We explicitly use this constraint to design a density loss to make the occupancy network dispatch points with small density values to the empty space network. This density loss can ensure the network predicts more accurate occupancy.

Our imbalanced occupancy loss and the density loss work together with the rendering loss, so that our network is more aware of the rendering quality. Our LeC²O-NeRF converges very fast in learning occupancy. After training the occupancy, we can utilize it to guide the point sampling in the state-of-the-art NeRF methods, such as Instant-NGP (Müller et al., 2022) and the large-scale Switch-NeRF (MI & Xu, 2023). We freeze the learned occupancy network and use it as an occupancy predictor. If a point is predicted as unoccupied, it is discarded and is not processed by the main NeRF network. In our experiments, we can consistently outperform the occupancy grid in terms of accuracy, and can successfully speed up state-of-the-art NeRF methods without sacrificing accuracy. Our method can also learn more compact, accurate and smooth occupancy compared to the occupancy grid. The smoothness is apparent as shown in the rendered videos in the supplementary.

2 RELATED WORK

NeRF. Neural Radiance Fields (Mildenhall et al., 2020) utilize a multilayer perceptron (MLP) network to encode a 3D scene from multi-view images. It has been extended to model a lot of tasks (Liu et al., 2020; Xu et al., 2022; Jaehyeok et al., 2024; Kerbl et al., 2023; Zhang et al., 2023a; Wang et al., 2023) or even city-level large-scale scenes (Turki et al., 2022; Tancik et al., 2022; Wang & Xu, 2024; MI & Xu, 2023; Qu et al., 2024). The main idea of these large-scale NeRF methods is to decompose the large-scale scene into partitions and use different sub-networks to encode different parts, and then compose the sub-networks. The Mega-NeRF (Turki et al., 2022) and Block-NeRF (Tancik et al., 2022) manually decompose the scene by distance or image distribution. The sub-networks are trained separately and composed with manually defined rules. The Switch-NeRF (MI & Xu, 2023) learns the scene decomposition by an MoE network and trains different experts in an end-to-end manner. There are also several methods (Xu et al., 2023; Zhang et al., 2023b; Zhong et al., 2024) employing the hash encoding (Müller et al., 2022) and plane encoding (Chan et al., 2022; Chen et al., 2022) while not decomposing the scene. In contrast to these existing works, our LeC²O-NeRF method focuses on learning the occupancy of a large-scale scene. The learned occupancy can be used to accelerate large-scale NeRF methods.

Occupancy and efficient sampling in NeRF. Many methods are proposed to estimate the important regions. NeRF (Mildenhall et al., 2020) trains a coarse and fine network together for hierarchical sampling. The Mip-NeRF 360 (Barron et al., 2022) designs a small proposal network to predict density and converts it into a sampling weight vector. Apart from these methods directly predicting the weight distributions, there are many methods (Müller et al., 2022; Fridovich-Keil et al., 2022; Tang et al., 2021; Hu et al., 2022; Li et al., 2022) use the binary occupancy for sampling. The NerfAcc (Li et al., 2022) provided a plug-and-play occupancy grid module and has shown in extensive experiments that estimating occupancy can greatly accelerate the training of various NeRF methods. The Instant-NGP (Müller et al., 2022) uses multi-scale occupancy grids to encode the occupancy. These existing methods using occupancy grids typically focus on small-scale scene modeling. The occupancy grid faces problems on large-scale scenes, as described above. In this paper, we focus on learning a continuous and compact occupancy representation for large-scale scenes.

3 THE PROPOSED METHOD

3.1 OVERVIEW

Our LeC²O-NeRF learns occupancy of a 3D scene end-to-end in the training of a Neural Radiance Field F . The framework is shown in Fig. 2. F takes a 3D point \mathbf{x} and its direction \mathbf{d} as input. It predicts the color \mathbf{c} and density σ for each \mathbf{x} . It contains an occupancy network, $n + 1$ sub-networks, and two prediction heads. The occupancy network O is an MLP classification network. It dispatches different points into different sub-networks. The scene network consists of the n sub-networks $\mathcal{S} = \{S_i, i = 1 \dots n\}$ and handles occupied points. The empty space network is a special

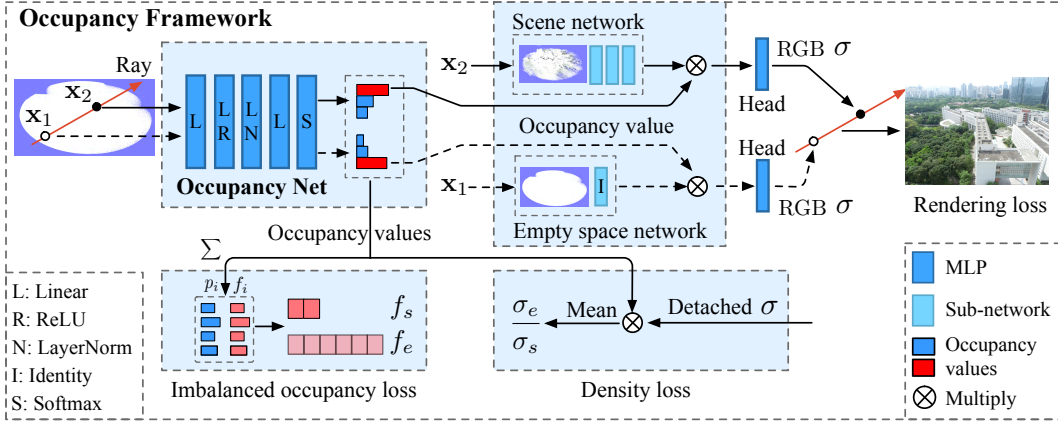


Figure 2: Our proposed LeC²O-NeRF. The occupancy network predicts the occupancy of each point and dispatches them into different sub-networks. \mathbf{x}_1 and \mathbf{x}_2 go through the occupancy network and are dispatched to the empty space network and the scene network, according to their occupancy values. The occupancy can be trained end-to-end together with the NeRF network by multiplying occupancy values on the output of sub-networks. If a point is dispatched into the empty space network, it is classified as unoccupied. The occupancy network is a small MLP. We enlarge the figure of the occupancy network to clearly show its operation. The imbalanced occupancy loss and the density loss are computed by the occupancy values and the detached σ .

tiny sub-network E_e to handle unoccupied points. The prediction head H_s and H_e are for \mathcal{S} and E_e , respectively. After training, the occupancy of the 3D scene is encoded in the occupancy network O and the radiance field is encoded in the scene and empty space networks.

A 3D point \mathbf{x} first goes through the occupancy network O and obtains $n+1$ occupancy values. These values correspond to the scene network’s n sub-networks and the empty space network. Then, \mathbf{x} is dispatched into only one of the $n+1$ sub-networks according to the occupancy values. If a scene sub-network is selected, it implies that \mathbf{x} is occupied. \mathbf{x} is then input to the scene MLP and the prediction head H_s . If the empty space network is selected, it implies that \mathbf{x} is not occupied. It then goes through E_e and H_e . Therefore, the occupancy network performs as a binary classification network to identify the occupied and unoccupied points. Our proposed imbalanced occupancy loss and the density loss are computed to train the occupancy network together with the volume rendering loss in NeRF (Mildenhall et al., 2020).

3.2 NETWORK STRUCTURE OF LEC²O-NeRF

Occupancy network. The occupancy network O in our LeC²O-NeRF serves as a classification network to dispatch 3D points into different sub-networks, as depicted in Fig. 2. O predicts a vector of $n+1$ normalized occupancy values $O(\mathbf{x})$ for a 3D point \mathbf{x} . The first n occupancy values correspond to the n scene sub-networks in \mathcal{S} . The last occupancy value corresponds to the empty space network E_e . We use Top-1 operation to obtain the index k of the Top-1 value in $O(\mathbf{x})$. Then, we dispatch \mathbf{x} into the sub-network of index k . The occupancy value is multiplied by the output of the sub-network. This allows gradients from the main rendering loss to be propagated backward through the occupancy network, enabling the occupancy network to be trained together with the entire network.

If \mathbf{x} is assigned to E_e , it implies that \mathbf{x} is unoccupied. It goes through E_e and H_e to predict density σ and color \mathbf{c} . If the assigned sub-network is one of the scene sub-networks, this indicates that \mathbf{x} is occupied. Then, \mathbf{x} goes through the corresponding scene sub-network and the head H_s to predict σ and \mathbf{c} . After training the entire network, the occupancy of a 3D scene is encoded into the compact occupancy network O . Then, we can use O as an occupancy predictor. An input point is unoccupied if the occupancy network dispatches it to E_e . In our implementation, the occupancy network contains 4 linear layers and a layer-norm layer.

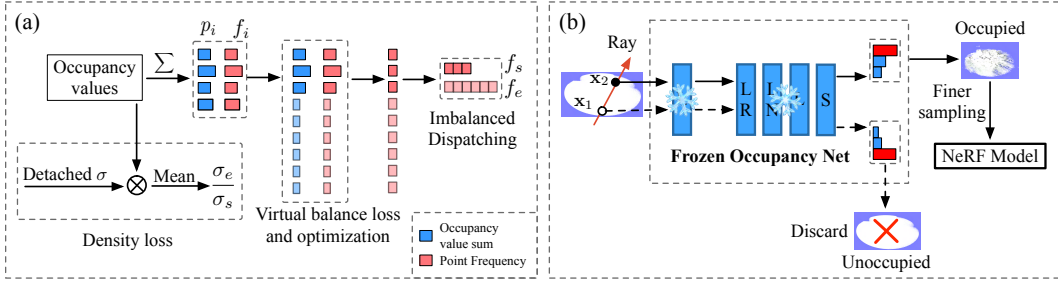


Figure 3: (a) The computation of the imbalanced occupancy loss and the density loss from occupancy values. (b) After training the occupancy network of a scene, we can use our frozen occupancy network to guide the sampling and training of NeRF methods.

Sub-networks and heads. The proposed LeC²O-NeRF is imbalanced because the sub-networks are different. The scene network $\mathcal{S} = \{S_i, i = 1 \dots n\}$ contains n sub-networks with the same architecture, each of which consists of 7 linear layers. They encode the occupied points. The prediction head H_s for \mathcal{S} is shared. H_s also accepts the view direction \mathbf{d} and appearance embedding AE (Martin-Brualla et al., 2021) as inputs to encode a view-dependent color. We use n sub-networks in the scene network in order to enlarge its network capacity for encoding large-scale scenes.

The empty space network E_e is defined as a *tiny* network to encode unoccupied (i.e. empty space) points. We use an identity layer to directly feed-forward the input into the prediction head H_e . The tiny E_e results in fewer parameters for empty space. As a result, E_e tends to predict smooth density and color values and therefore favors the unoccupied points whose density is small and smooth. The scene network \mathcal{S} is designed to contain much more network parameters than E_e , because occupied points contain significantly more important information.

3.3 LARGE-SCALE OCCUPANCY OPTIMIZATION LOSSES

The occupancy network and imbalanced network structure cannot naturally learn reasonable occupancy without priors of the 3D scene. We further propose an imbalanced occupancy loss and a density loss to regularize the occupancy network to learn accurate occupancy for a large-scale scene, as depicted in Fig. 3(a).

Imbalanced occupancy loss. In a 3D scene, the occupied and unoccupied 3D points are naturally imbalanced. A large portion of the 3D scene points is unoccupied. Our empty space network O should secure more 3D points to faithfully learn the imbalanced nature of the scene. To accomplish the imbalanced classification, we design an imbalanced occupancy loss L_o to directly control the portions of occupied and unoccupied points during the training. This loss not only can dispatch more points into E_e , but also can keep the number of points roughly the same for each scene sub-network. This means that L_o is imbalanced for the empty space network while balanced for the scene sub-networks.

Our imbalanced occupancy loss is inspired by the balanced loss L_b in (Lepikhin et al., 2021). We first introduce this balanced loss. It aims to dispatch a similar number of points to each sub-network. Let n be the number of total sub-networks, and f_i be the fraction of points dispatched into sub-network i . Then, $\sum f_i^2$ is minimized if all f_i are equal. However, $\sum f_i^2$ is not differentiable, so it cannot be used as a loss function. As shown in (Lepikhin et al., 2021), it replaces one f_i by a soft version p_i , where p_i is the fraction of the occupancy values dispatched to sub-network i . Therefore, the balanced loss can be defined as $L_b = n \sum_{i=1}^n f_i p_i$. Under the optimal balance dispatching, L_b will be 1. Inspired by L_b , we define the imbalanced occupancy loss L_o . We can consider the empty space network E_e as v virtual sub-networks. The fraction of each virtual sub-network is thus f_e/v , and the fraction of the occupancy values is p_e/v . Then, we can compute the balanced loss for the v virtual sub-network and the n scene sub-networks. When $n + v$ sub-networks are balanced, E_e can

obtain more points. Hence, we define L_o as:

$$L_o = (n + v) \left(v \frac{f_e p_e}{v} + \sum_{i=1}^n f_i p_i \right) = (n + v) \left(\frac{f_e p_e}{v} + \sum_{i=1}^n f_i p_i \right) \quad (1)$$

When optimal dispatching is achieved, E_e obtains a portion of $v/(n + v)$ points. Each scene sub-network obtains a portion of $1/(n + v)$. L_o is 1.0. Therefore, L_o can approximately control the ratio of occupied and unoccupied points. We typically set $n = 8$, $v = 80$ in our experiments. These values make the occupancy network dispatch about 85% points to the empty space network.

Density loss. We design a density loss to explicitly guide the occupancy network O to learn better occupancy. Our main idea is that the average density of the points dispatched to the empty space sub-network E_e should be much smaller than that of the scene network \mathcal{S} . Let the set of points dispatched to E_e and \mathcal{S} be \mathcal{X} and \mathcal{Y} , respectively. The average density σ_e of E_e is $\sigma_e = \frac{1}{|\mathcal{X}|} \sum_{i \in \mathcal{X}} \sigma_i$. The average density σ_s for \mathcal{S} is $\sigma_s = \frac{1}{|\mathcal{Y}|} \sum_{i \in \mathcal{Y}} \sigma_i$. Then, the ratio σ_e/σ_s should be small if the occupancy is learned correctly. The problem is that the σ_e/σ_s cannot affect the occupancy network. Therefore, we include the occupancy values in the computation of the mean density. The σ_e and σ_s can be rewritten as $\sigma_e = \frac{1}{|\mathcal{X}|} \sum_{i \in \mathcal{X}} o_i \sigma_i$ and $\sigma_s = \frac{1}{|\mathcal{Y}|} \sum_{i \in \mathcal{Y}} o_i \sigma_i$. The value o_i used for a point of the scene network is the sum of the occupancy values for the n scene sub-networks. Therefore, the density loss L_d can be defined as:

$$L_d = \frac{\sigma_e}{\sigma_s} = \frac{|\mathcal{Y}| \sum_{i \in \mathcal{X}} o_i \sigma_i}{|\mathcal{X}| \sum_{i \in \mathcal{Y}} o_i \sigma_i} \quad (2)$$

We detach σ when computing L_d . When L_d is large, it optimizes the output of the occupancy network to make it dispatch correctly.

Rendering loss. Our network learns the occupancy during the training of NeRF. Therefore, our main optimization loss is the rendering loss (Mildenhall et al., 2020). We sample N 3D points along a ray \mathbf{r} and predict the density σ_i and color \mathbf{c}_i for each 3D point \mathbf{x}_i by the network. We use σ_i to compute $\alpha_i = 1 - \exp(-\sigma_i \delta_i)$, where δ_i is the distance of two nearby points. Then, we compute the transmittance $T_i = \exp(-\sum_{j=1}^{i-1} \sigma_j \delta_j)$ of \mathbf{x}_i along the ray. The predicted color $\hat{C}(\mathbf{r})$ is computed as $\hat{C}(\mathbf{r}) = \sum_{i=1}^N T_i \alpha_i \mathbf{c}_i$. The rendering loss L_r is computed by $\hat{C}(\mathbf{r})$ and the ground-truth color $C(\mathbf{r})$.

Let the set of rays be \mathcal{R} . L_r is defined as $L_r = \sum_{r \in \mathcal{R}} \left\| \hat{C}(\mathbf{r}) - C(\mathbf{r}) \right\|_2^2$.

Final loss. The final loss L_f is the weighted sum of L_r , L_o and L_d . $L_f = w_r L_r + w_o L_o + w_d L_d$, where w_r , w_o , and w_d are corresponding loss weights.

3.4 LARGE-SCALE OCCUPANCY AS GUIDANCE

When training the occupancy network, unoccupied points still need gradients for optimization, which consumes memory and computation. Since our occupancy network converges very fast, we can freeze it after it converges and use it to filter unoccupied points for a NeRF network, as shown in Fig. 3(b). O is much smaller than the main NeRF network, so the training can be significantly accelerated.

In the guided training, we first sample a set of coarse samples and send them into the frozen occupancy network O to discard unoccupied points, typically 85% points from our observation. Then, we split the reserved samples to obtain finer samples. These two steps can reduce the number of points sent into O . In the experiments, we typically sample 128 samples along a ray and use the occupancy to filter the samples and split each occupied sample into 8 new samples.

4 EXPERIMENTS

4.1 DATASETS

We use two publicly available large-scale datasets for evaluation. The Mega-NeRF dataset (Turki et al., 2022) consists of the Building, Rubble, Residence, Sci-Art, and Campus scenes. Each of them contains from $2k$ to $6k$ images with a resolution of about $5k \times 3k$. The Block-NeRF dataset (Tancik et al., 2022) contains a scene with $12k$ images with a resolution of about $1k \times 1k$.

Table 1: Accuracy, Precision, Recall, F1-Score, parameter number, and occupancy ratio of different occupancy methods. Our method clearly outperforms the occupancy grid with more compact parameter sizes and better occupancy ratios.

Dataset	Sci-Art		Campus		Rubble		Building		Residence	
Method	Grid	Ours	Grid	Ours	Grid	Ours	Grid	Ours	Grid	Ours
Accuracy	0.912	0.904	0.619	0.684	0.697	0.712	0.521	0.711	0.656	0.703
Precision	0.315	0.339	0.371	0.437	0.269	0.319	0.183	0.322	0.232	0.314
Recall	0.519	0.795	0.746	0.883	0.666	0.914	0.549	0.683	0.634	0.958
F1-Score	0.392	0.476	0.496	0.584	0.383	0.473	0.274	0.438	0.339	0.473
Para. Number	2.0M	0.15M	2.0M	0.15M	2.0M	0.15M	2.0M	0.15M	2.0M	0.15M
Occupancy ratio	22.8%	13.0%	34.0%	14.5%	33.6%	13.0%	44.0%	15.0%	37.5%	15.9%

4.2 METRICS AND VISUALIZATION

We evaluate the occupancy accuracy with Occupancy Metrics and apply the occupancy on the sampling of state-of-the-art NeRF methods (Müller et al., 2022; MI & Xu, 2023) to compute the Image Reconstruction Metrics.

Occupancy metrics. We evaluate the occupancy classification accuracy. The ground-truth occupancy is usually not available in real-world large-scale NeRF datasets. As a fully-trained NeRF without using occupancy can obtain a good estimation of the geometry of the scene, we use it as a good reference for evaluation. We extract depth maps predicted by the large-scale Switch-NeRF (MI & Xu, 2023) and convert them into an occupancy grid. Then, we also convert our learned occupancy into another occupancy grid by sampling and evaluating point occupancy. The occupancy accuracy is computed by comparing the converted occupancy grids.

Image reconstruction metrics. We use our learned occupancy to guide the training of several representative NeRF methods, including Instant-NGP (INGP) (Müller et al., 2022) and the large-scale Switch-NeRF (MI & Xu, 2023). We use PSNR, SSIM (Wang et al., 2004) (both higher is better), and LPIPS (Zhang et al., 2018) (lower is better) to evaluate the validation images.

Occupancy visualization. We visualize the occupancy as point clouds. We sample and merge 3D points of rays in the validation images. These point clouds are visualized by two methods. The first one is to directly visualize the predicated color of each point. The second one uses the $\alpha = 1 - \exp(-\sigma_i \delta_i)$ as an additional channel to show the color and transparency of the point clouds. The unoccupied points should be largely transparent. The two visualization methods complement each other for better visualization of the occupancy.

4.3 IMPLEMENTATION DETAILS

When training the occupancy network on the Mega-NeRF dataset, we use 8 sub-networks for the scene network. The occupancy network contains one input layer, two inner layers, one layer-norm layer, and one output layer. The channel number of the main layers is set as 256. The empty space network is an identity layer. We set $w_r = 1.0$, $w_o = 0.0005$, $w_d = 0.1$ and $v = 80$. We sample 512 points for each ray. We train the occupancy for 40k steps. The training of the occupancy network takes from 1.6h to 1.8h. The learning rate is set as 5×10^{-4} . When training the occupancy network on the Block-NeRF dataset, we use Mip embedding proposed in (Barron et al., 2021). w_d is set as 0.005 and v is set as 40.

When applying our learned occupancy network on NeRF methods such as the Instant-NGP (INGP) (Müller et al., 2022) and Switch-NeRF (MI & Xu, 2023), we use the occupancy network to guide their sampling. To compare with the occupancy grid, we employ the OccGridEstimator from NeRFacc (Li et al., 2022). The grid size is set as the default (i.e., 128^3). The OccGridEstimator is updated with the main network. The main results are obtained by training on 2 NVIDIA RTX 3090 GPUs for INGP and 8 NVIDIA RTX 3090 GPUs for Switch-NeRF. We sample 8192 rays for the Mega-NeRF dataset and 13312 rays for the Block-NeRF dataset. We align the training time of our methods with the grid methods trained with 500k iterations.

4.4 BENCHMARK PERFORMANCE

Occupancy Metrics. We evaluate our occupancy accuracy with the Occupancy Metrics. Since the unoccupied and occupied points are highly imbalanced, we report the Accuracy, Precision, Recall, and F1-Score to complement each other. In Table 1, our learned occupancy can clearly outperform the Occupancy Grid in almost all the metrics on all Mega-NeRF scenes, with clearly more compact parameter sizes. Notably, our network is much better on Recall, indicating that it is good at correctly predicting the occupied points, which is critical for better NeRF optimization. The occupancy ratio in Table 1 means the ratio of occupied points to go through the main NeRF. Our occupancy network also retains fewer points than the occupancy grid while achieving better accuracy. These results demonstrate that our method can predict more accurate and compact occupancy.

Image Reconstruction Metrics. Table 2 shows the results of applying our learned occupancy on Instant-NGP (INGP) (Müller et al., 2022) and Switch-NeRF (MI & Xu, 2023) on Block-NeRF dataset. Our method significantly surpasses both Instant-NGP (Müller et al., 2022) (INGP) and Switch-NeRF with an occupancy grid (Switch+Grid) in terms of PSNR, with margins of **2.36** and **0.84**, respectively. Given the substantial size of Block-NeRF dataset, which comprises $12k$ images, the results highlight the superiority of our method when compared to the occupancy grid method. Note that the training time of our method includes our occupancy training time for fair comparisons.

Table 2: The image accuracy on Block-NeRF dataset (Tancik et al., 2022). INGP+Ours outperforms INGP (Müller et al., 2022) by a PSNR of **2.36**. Switch+Ours not only outperforms Switch-NeRF (MI & Xu, 2023), but also outperforms Switch+Grid by a PSNR of **0.84**. INGP-based methods are trained with 20.0h. Switch-NeRF-based methods are trained with 24.0h.

Method	PSNR \uparrow	SSIM \uparrow	LPIPS \downarrow
INGP	19.49	0.701	0.558
INGP+Ours	21.85	0.738	0.507
Switch	22.85	0.742	0.515
Switch+Grid	22.26	0.740	0.511
Switch+Ours	23.10	0.751	0.498

Table 3: The accuracy and training time on Mega-NeRF dataset (Turki et al., 2022). Our method on Instant-NGP (NGP+Ours) clearly outperforms the occupancy grid INGP (Müller et al., 2022). Our method on Switch-NeRF (Switch+Ours) clearly outperform Switch+Grid and Switch-NeRF (Switch) (MI & Xu, 2023). The occupancy grid cannot successfully speed up the training without decreasing the accuracy. Switch-NeRF-based methods are trained by 13.6h. NGP-based methods are trained by 11.6h.

Dataset	Sci-Art			Campus			Rubble			Building			Residence		
	Metric	PSNR \uparrow	SSIM \uparrow	LPIPS \downarrow	PSNR \uparrow	SSIM \uparrow	LPIPS \downarrow	PSNR \uparrow	SSIM \uparrow	LPIPS \downarrow	PSNR \uparrow	SSIM \uparrow	LPIPS \downarrow	PSNR \uparrow	SSIM \uparrow
Switch	25.46	0.762	0.400	22.76	0.507	0.659	23.58	0.519	0.546	20.50	0.517	0.526	21.77	0.611	0.501
Switch+Grid	25.48	0.760	0.413	22.75	0.500	0.671	23.69	0.522	0.549	20.33	0.495	0.547	22.18	0.622	0.500
Switch+Ours	26.04	0.772	0.398	23.21	0.517	0.635	23.96	0.548	0.516	20.64	0.522	0.517	22.10	0.626	0.485
NGP	23.98	0.724	0.445	21.76	0.475	0.677	22.94	0.498	0.572	19.48	0.454	0.585	21.27	0.591	0.515
NGP+Ours	24.50	0.754	0.412	22.83	0.518	0.623	23.66	0.558	0.501	20.33	0.511	0.518	21.77	0.626	0.473

Table 3 shows the results of Switch-NeRF (Switch) (MI & Xu, 2023), Switch-NeRF with an occupancy grid (Switch+Grid), Switch-NeRF with our learned occupancy network (Switch+Ours), Instant-NGP (INGP) (Müller et al., 2022), and Instant-NGP with our learned occupancy network (INGP+Ours), on the Mega-NeRF dataset (Turki et al., 2022). Instant-NGP (Müller et al., 2022) already incorporates an occupancy grid to guide the training. We align the training time to the grid-based methods. Note that we include the occupancy training time in Switch+Ours and NGP+Ours for a fair comparison.

We highlight the best values among Switch, Switch+Grid, and Switch+Ours, and the best values between NGP and NGP+Ours. As shown in Table 3, our method consistently outperforms Switch, NGP, and Switch+Grid. Therefore, our method is significant to speed up the training of Switch-NeRF and NGP while achieving superior accuracy. Notably, the Switch+Grid does not obtain better results than Switch-NeRF. This means that on a challenging large-scale scene, the occupancy grid cannot successfully speed up the training without sacrificing accuracy. In contrast, our occupancy network can largely improve the accuracy. We visualize the point clouds of occupancy in Fig. 4. The point clouds show that our network can learn more compact and clean occupancy than the occupancy grid. We also provide the visualization comparison of rendered images in Fig. 5 and a video in the supplementary files.

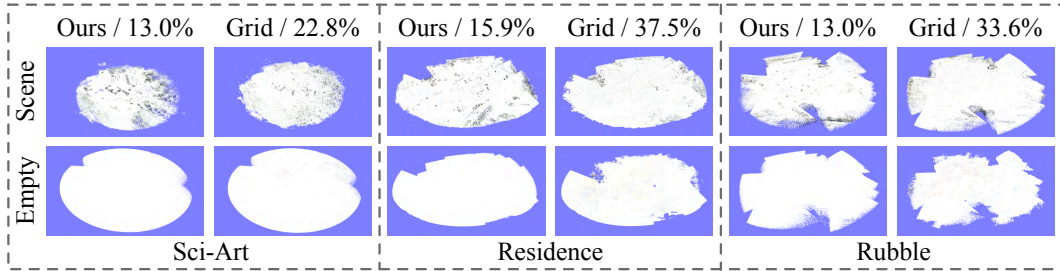


Figure 4: The visualization of our occupancy and the grid occupancy as point clouds. Our predicted occupied points (scene surface points) are cleaner and have fewer points than the grid occupancy. They fit the surface of the buildings more compactly.

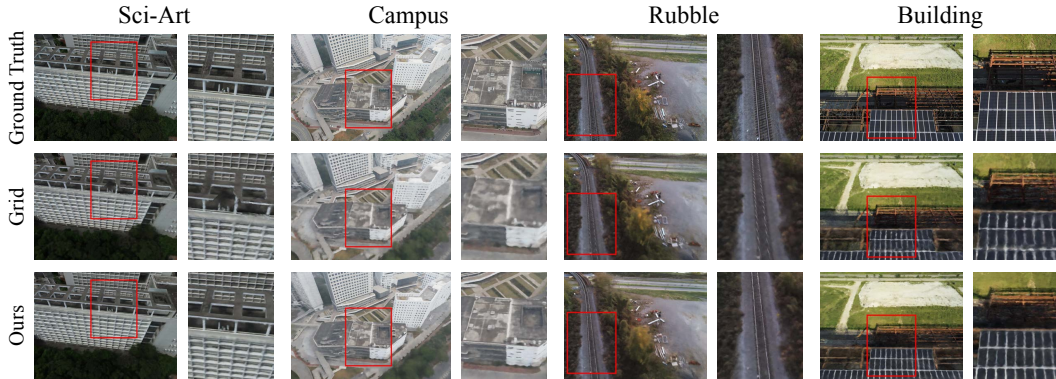


Figure 5: The rendered images of our occupancy network and the occupancy grid based on Switch-NeRF. Our method can obtain more complete, clean, and high-quality images.

4.5 ABLATION STUDY

In this section, we perform several ablations to analyze the designs of our imbalanced network structure, the density loss, and the learned occupancy. The experiments are performed by applying our occupancy on Switch-NeRF and the Sci-Art scene for 40K occupancy steps and 500K NeRF steps if not specified.

Table 4: Ablation on the structure of E_e **with** occupancy loss L_o **without** the density loss L_d . 7-layer, 4-layer, and Identity mean using a 7-layer MLP, a 4-layer MLP, or an Identity layer in the empty space network. Larger empty space networks cannot learn reasonable occupancy, while our imbalanced structure with an Identity layer can learn good occupancy.

Method	PSNR \uparrow	SSIM \uparrow	LPIPS \downarrow
7-layer	20.23	0.631	0.506
4-layer	23.62	0.701	0.463
Identity	26.30	0.781	0.383

Table 5: Ablation study on the memory usage and accuracy of our method and the occupancy grids with different resolutions. With a resolution of 256^3 (Grid-256), the occupancy grid method slows down dramatically and obtains much worse accuracy than ours trained with the same time. Moreover, Grid-256 consumes about $4.5\times$ memory than our method. All methods are trained with 14.1h.

Method	PSNR \uparrow	SSIM \uparrow	LPIPS \downarrow	Mem. \downarrow
Switch-NeRF	25.46	0.762	0.400	10.5G
Grid-128	25.48	0.760	0.413	5.8G
Grid-256	24.75	0.728	0.448	12.5G
Ours	26.04	0.772	0.398	2.7G

Imbalanced network structure. We perform experiments to show that our designed imbalanced network structure with the imbalanced occupancy loss can learn the occupancy. We set the empty space network E_e to different network sizes. 7-layer means using a 7-layer MLP in E_e , the same as the scene sub-networks, creating a balanced structure. 4-layer uses a smaller 4-layer MLP in

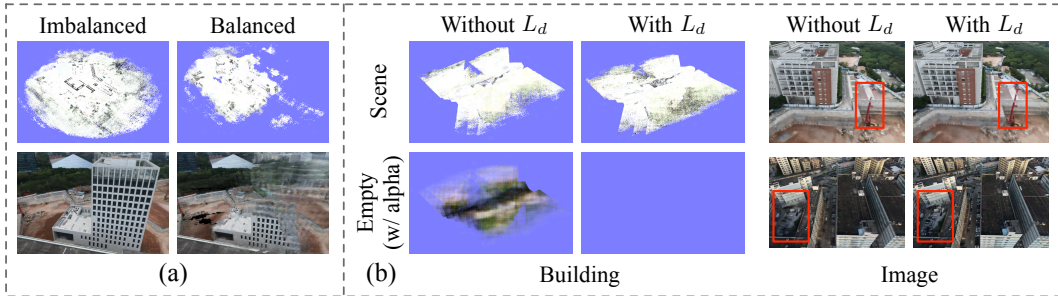


Figure 6: (a) The occupied points and images with the imbalanced and balanced networks. Our imbalanced network learns complete occupancy and images. The balanced structure cannot distinguish the occupied and unoccupied regions. (b) Point clouds of the scene network and the empty space network with and without the density loss. We visualize the point clouds of the empty space network with transparency related to alpha values (see Sec. 4.2) to better show whether the points are empty or not. With L_d , our imbalanced structure can learn better occupancy and thus the points of E_e are all transparent. With L_d , the images are more complete in challenging regions.

E_e . Identity means that we use an identity layer in E_e , which is our proposed imbalanced network structure.

As shown in Table 4, the rendering accuracy of the 7-layer balanced structure largely dropped compared to our imbalanced empty space network with an Identity layer. Our imbalanced structure can obtain reasonable accuracy. Note that the imbalanced occupancy loss is used while the density loss is **not** used in these experiments. As shown in Fig. 6(a), the scene network of our imbalanced structure handles the full occupied points. The scene network of the balanced structure only handles a part of the occupied points. This means that the balanced structure cannot learn reasonable occupancy, and its rendered image is thus of low quality. These experiments show that, to implicitly model the imbalanced occupancy of a 3D scene, it is important to design an imbalanced network.

Density loss. We ablate on the density loss L_d on the Building scene in Table 6. Our full method achieves better accuracy than that without the density loss. As shown in Fig. 6(b), with L_d , the network can separate the occupied and unoccupied points more clearly, and the rendered images contain fewer artifacts in the challenging regions. These experiments show that, our density loss can provide more explicit information to the occupancy network and make the occupancy network learn more accurate occupancy.

Table 6: Ablation on the density loss L_d on the Building scene. L_d can help our occupancy network learn better occupancy and achieve better accuracy.

Method	PSNR \uparrow	SSIM \uparrow	LPIPS \downarrow
Ours w/o l_d	20.59	0.516	0.521
Ours	20.79	0.531	0.508

Memory usage. We analyze the memory usage and the accuracy of our method, and the occupancy grids with different resolutions to better demonstrate the advantages of our compact occupancy network. As shown in Table 5, our method has the lowest memory usage compared to Switch-NeRF (MI & Xu, 2023) and occupancy grids with resolutions of 128^3 (Grid-128) and 256^3 (Grid-256). Notably, Switch-NeRF (MI & Xu, 2023) and Grid-256 consume about $4.5\times$ more memory than ours while still achieving inferior results. The Grid-256 slows down dramatically than Grid-128 and obtains worse results when trained with the same time. This study clearly shows the advantage of the compactness of our proposed occupancy network.

Occupancy analysis. We analyze the occupancy statistics related to the points of the scene network and the empty space network with respect to the occupancy training steps on the evaluation images of the Sci-Art scene in Fig. 8. Fig. 8a is the portion of points in the scene network S and the empty space network E_e of different training steps. There are consistently more than 80% points in E_e . This figure verifies the effectiveness of our imbalanced occupancy loss. It also shows that we can speed up the training largely if we use the learned occupancy to guide the sampling of points. Fig. 8b and Fig. 8c show mean density values and alpha values of the points in S and E_e . The points of S

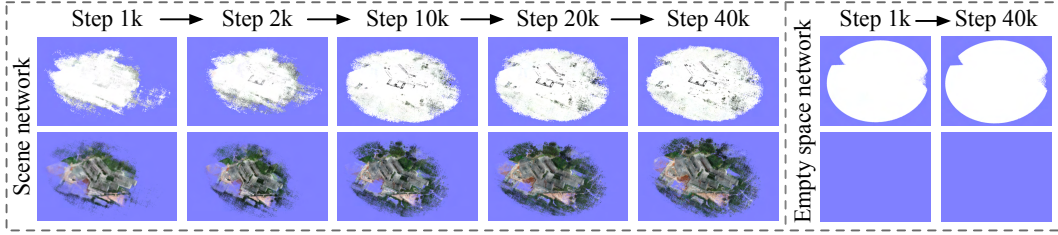


Figure 7: The point clouds dispatched to the scene network and the empty space network at each step. The scene network converges fast to the whole occupied area. The points in the empty space network consistently have very small opacity, resulting empty figures for the point cloud of the empty space network. Our network can learn accurate occupancy with only 20k to 40k steps. The two rows visualize the point clouds without and with transparency respectively as described in Sec. 4.2.

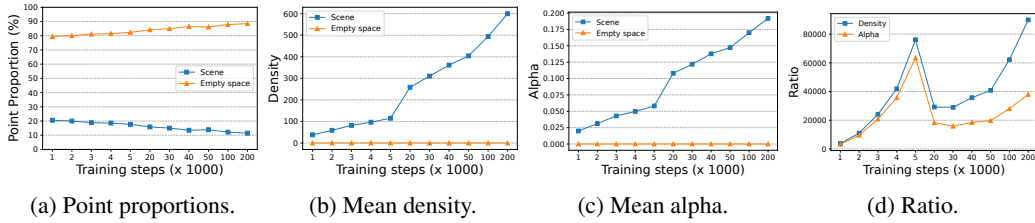


Figure 8: The statistics of the scene network \mathcal{S} and the empty space network E_e at different training steps. (a) The portion of the points in \mathcal{S} and E_e . (b) (c) The mean density values and alpha values of the points in \mathcal{S} and E_e . (d) The density value ratio and alpha value ratio between the points in \mathcal{S} and E_e .

have clearly much larger densities and alpha values than those of E_e . The values of points in E_e are nearly zero. This indicates that our network can effectively dispatch points according to their densities. Fig. 8d shows the density value ratio and the alpha value ratio between points in \mathcal{S} and E_e . The values of points in \mathcal{S} are several magnitudes larger than those in E_e . As the ratios are the direct target of the density loss, they can fully validate the effectiveness of our designed density loss.

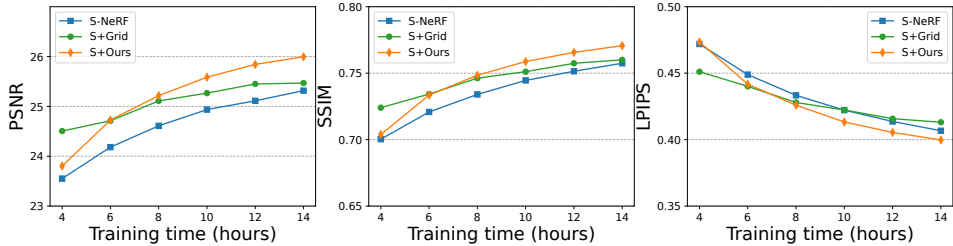


Figure 9: Analysis of training time and accuracy: our method (S+Ours) demonstrates remarkable convergence speed when compared to the grid-based occupancy (S+Grid) and the original Switch-NeRF (S-NeRF) (MI & Xu, 2023) on Sci-Art. Note that the training time of our method includes the training time of our occupancy network.

Fig. 7 visualizes the point clouds dispatched to the scene network and the empty space network. The points in the scene network have larger opacity. They cover the whole scene surface quickly only after 10k steps of training. The points in the empty space network consistently present very small opacity, indicating that they are empty. The first row visualizes the points without transparency and the second row visualizes the points with transparency.

The extensive analysis of the occupancy clearly shows that the proposed LeC²O-NeRF can learn the occupancy of a large-scale 3D scene accurately and quickly. It can be effectively encoded via our compact occupancy network.

Accuracy of different training times. We analyze the detailed accuracy of our method on Sci-Art with respect to the training time in Fig. 9. Our method on Switch-NeRF (S+Ours) demonstrates remarkable convergence speed compared to the grid-based occupancy on Switch-NeRF (S+Grid) and the original Switch-NeRF (MI & Xu, 2023) (S-NeRF). Note that the training time of our method in this figure already includes the training time of our occupancy network.

5 CONCLUSION

In this paper, we have proposed LeC²O-NeRF to learn continuous and compact occupancy for large-scale scenes. We achieve this by our core designs of a compact occupancy network, an imbalanced occupancy loss, a novel imbalanced network structure, and a density loss. Experiments on challenging large-scale datasets have shown that our learned occupancy clearly outperforms the occupancy grid and can achieve superior accuracy with much less time. Since occupancy is a very important concept in many 3D research areas, this work will offer more inspiration to the research of learning and representation of occupancy.

REFERENCES

- Jonathan T. Barron, Ben Mildenhall, Matthew Tancik, Peter Hedman, Ricardo Martin-Brualla, and Pratul P. Srinivasan. Mip-nerf: A multiscale representation for anti-aliasing neural radiance fields. *ICCV*, 2021.
- Jonathan T. Barron, Ben Mildenhall, Dor Verbin, Pratul P. Srinivasan, and Peter Hedman. Mip-nerf 360: Unbounded anti-aliased neural radiance fields. In *CVPR*, 2022.
- Eric R. Chan, Connor Z. Lin, Matthew A. Chan, Koki Nagano, Boxiao Pan, Shalini De Mello, Orazio Gallo, Leonidas Guibas, Jonathan Tremblay, Sameh Khamis, Tero Karras, and Gordon Wetzstein. Efficient geometry-aware 3D generative adversarial networks. In *CVPR*, 2022.
- Anpei Chen, Zexiang Xu, Andreas Geiger, Jingyi Yu, and Hao Su. Tensorf: Tensorial radiance fields. In *ECCV*, 2022.
- Sara Fridovich-Keil, Alex Yu, Matthew Tancik, Qinhong Chen, Benjamin Recht, and Angjoo Kanazawa. Plenoxels: Radiance fields without neural networks. In *Proceedings of the IEEE/CVF Conference on Computer Vision and Pattern Recognition (CVPR)*, pp. 5501–5510, June 2022.
- Tao Hu, Shu Liu, Yilun Chen, Tiancheng Shen, and Jiaya Jia. Efficientnerf efficient neural radiance fields. In *CVPR*, 2022.
- Kim Jaehyeok, Wee Dongyoon, and Dan Xu. Motion-oriented compositional neural radiance fields for monocular dynamic human modeling. In *ECCV*, 2024.
- Bernhard Kerbl, Georgios Kopanas, Thomas Leimkühler, and George Drettakis. 3d gaussian splatting for real-time radiance field rendering. *ACM Transactions on Graphics*, 42(4), July 2023. URL <https://repo-sam.inria.fr/fungraph/3d-gaussian-splatting/>.
- Dmitry Lepikhin, HyoukJoong Lee, Yuanzhong Xu, Dehao Chen, Orhan Firat, Yanping Huang, Maxim Krikun, Noam Shazeer, and Zhifeng Chen. Gshard: Scaling giant models with conditional computation and automatic sharding. In *ICLR*, 2021.
- Ruilong Li, Matthew Tancik, and Angjoo Kanazawa. Nerfacc: A general nerf acceleration toolbox. *arXiv preprint arXiv:2210.04847*, 2022.
- Lingjie Liu, Jiatao Gu, Kyaw Zaw Lin, Tat-Seng Chua, and Christian Theobalt. Neural sparse voxel fields. *NeurIPS*, 2020.

-
- Ricardo Martin-Brualla, Noha Radwan, Mehdi SM Sajjadi, Jonathan T Barron, Alexey Dosovitskiy, and Daniel Duckworth. Nerf in the wild: Neural radiance fields for unconstrained photo collections. In *CVPR*, 2021.
- Zhenxing MI and Dan Xu. Switch-nerf: Learning scene decomposition with mixture of experts for large-scale neural radiance fields. In *The Eleventh International Conference on Learning Representations*, 2023. URL <https://openreview.net/forum?id=PQ2zoIZqvm>.
- Ben Mildenhall, Pratul P. Srinivasan, Matthew Tancik, Jonathan T. Barron, Ravi Ramamoorthi, and Ren Ng. Nerf: Representing scenes as neural radiance fields for view synthesis. In *ECCV*, 2020.
- Thomas Müller, Alex Evans, Christoph Schied, and Alexander Keller. Instant neural graphics primitives with a multiresolution hash encoding. *ACM Trans. Graph.*, 41(4):102:1–102:15, 2022.
- Delin Qu, Chi Yan, Dong Wang, Jie Yin, Qizhi Chen, Dan Xu, Yiting Zhang, Bin Zhao, and Xuelong Li. Implicit event-rgb neural slam. In *CVPR*, 2024.
- Matthew Tancik, Vincent Casser, Xinchen Yan, Sabeek Pradhan, Ben Mildenhall, Pratul P. Srinivasan, Jonathan T. Barron, and Henrik Kretzschmar. Block-nerf: Scalable large scene neural view synthesis. In *CVPR*, 2022.
- Jiapeng Tang, Jiabao Lei, Dan Xu, Feiying Ma, Kui Jia, and Lei Zhang. Sign-agnostic conet: Learning implicit surface reconstructions by sign-agnostic optimization of convolutional occupancy networks. In *ICCV*, 2021.
- Haithem Turki, Deva Ramanan, and Mahadev Satyanarayanan. Mega-nerf: Scalable construction of large-scale nerfs for virtual fly-throughs. In *CVPR*, 2022.
- Yuxin Wang, Wayne Wu, and Dan Xu. Learning unified decompositional and compositional nerf for editable novel view synthesis. In *ICCV*, 2023.
- Zhou Wang, Alan C Bovik, Hamid R Sheikh, and Eero P Simoncelli. Image quality assessment: from error visibility to structural similarity. *IEEE transactions on image processing*, 2004.
- Zipeng Wang and Dan Xu. Pygs: Large-scale scene representation with pyramidal 3d gaussian splatting. *arXiv preprint arXiv:2405.16829*, 2024.
- Linning Xu, Yuanbo Xiangli, Sida Peng, Xingang Pan, Nanxuan Zhao, Christian Theobalt, Bo Dai, and Dahua Lin. Grid-guided neural radiance fields for large urban scenes. In *CVPR*, 2023.
- Qiangeng Xu, Zexiang Xu, Julien Philip, Sai Bi, Zhixin Shu, Kalyan Sunkavalli, and Ulrich Neumann. Point-nerf: Point-based neural radiance fields. In *Proceedings of the IEEE/CVF Conference on Computer Vision and Pattern Recognition*, pp. 5438–5448, 2022.
- Richard Zhang, Phillip Isola, Alexei A Efros, Eli Shechtman, and Oliver Wang. The unreasonable effectiveness of deep features as a perceptual metric. In *CVPR*, 2018.
- Xiaoshuai Zhang, Abhijit Kundu, Thomas Funkhouser, Leonidas Guibas, Hao Su, and Kyle Genova. Nerflets: Local radiance fields for efficient structure-aware 3d scene representation from 2d supervision. *CVPR*, 2023a.
- Yuqi Zhang, Guanying Chen, and Shuguang Cui. Efficient large-scale scene representation with a hybrid of high-resolution grid and plane features. *arXiv preprint arXiv:2303.03003*, 2023b.
- Yingji Zhong, Lanqing Hong, Zhenguo Li, and Dan Xu. Cvt-xrf: Contrastive in-voxel transformer for 3d consistent radiance fields from sparse inputs. In *CVPR*, 2024.